J. Geomag. Geoelectr., **44**, 1225-1237, 1992

Dynamics Explorer Measurements of Particles, Fields, and Plasma Drifts Over a Horse-Collar Auroral Pattern

J. R. SHARBER[1], E. W. HONES, Jr.[2], R. A. HEELIS[3], J. D. CRAVEN[4], L. A. FRANK[5], N. C. MAYNARD[6], J. A. SLAVIN[7], and J. BIRN[2]

[1]*Southwest Research Institute, San Antonio, TX 78228, U.S.A.*
[2]*Los Alamos National Laboratory, Los Alamos, NM 87545, U.S.A.*
[3]*University of Texas at Dallas, Richardson, TX 75083, U.S.A.*
[4]*University of Alaska Fairbanks, Fairbanks, AK 99775, U.S.A.*
[5]*University of Iowa, Iowa City, IA 52242, U.S.A.*
[6]*Phillips Laboratory, Hanscom AFB, MA 01731, U.S.A.*
[7]*Goddard Space Flight Center, Greenbelt, MD 20771, U.S.A.*

(Received January 29, 1992; Accepted May 28, 1992)

As shown from ground-based measurements and satellite-borne imagers, one type of global auroral pattern characteristic of quiet (usually northward IMF) intervals is that of a contracted but thickened emission region in which the dawn and dusk portions can spread poleward to very high latitudes. Because of its shape, such a pattern has been referred to as a "horse-collar" aurora (HONES *et al.*, 1989). In this report we use the Dynamics Explorer data set to examine a case in which this "horse-collar" pattern was observed by the DE-1 auroral imager while at the same time DE-2, at lower altitude, measured precipitating particles, electric and magnetic fields, and plasma drifts. Our analysis shows that in general there is close agreement between the optical signatures and the particle precipitation patterns. In many instances, over scales ranging from tens to a few hundred kilometers, electron precipitation features and upward field-aligned currents are observed at locations where the plasma flow gradients indicate negative $\nabla \cdot \boldsymbol{E}$. The particle, plasma, and field measurements made along the satellite track and the 2-D perspective of the imager provide a means of determining the configuration of convective flows in the high-latitude ionosphere during this interval of northward IMF. Recent mapping studies are used to relate the low-altitude observations to possible magnetospheric source regions.

1. Introduction

The spatial distribution of auroral emissions at polar latitudes is much different during geomagnetically quiet conditions (i.e., when the IMF has a northward z-component) from that observed during intervals of moderate or strong geomagnetic activity. During nonquiet intervals auroras occupy a ringlike region of about 20° in radius, sometimes referred to as the instantaneous auroral oval, that surrounds an approximately circular polar cap within which auroras are not seen. But during quiet times auroras do occur in this central region and these typically take the form of sun-aligned arcs. The arcs are not uniformly or randomly distributed over the polar cap. From a statistical analysis of ground-based observations of auroras, LASSEN and DANIELSEN (1978) reported that a "polar cap pattern of discrete arcs" exists when the IMF B_z is positive and that it resides preferentially to the dawnward side of the magnetic pole

regardless of the sign of IMF B_y. Using the auroral mapping capability and precipitating particle measurements by DMSP satellites, MENG (1981) found that the pattern of sun-aligned arcs was seen on both the dawn and dusk sides of the pole and concluded that they signified a poleward extension of the dawn and dusk sides of the oval auroras to very high latitudes during quiescent geomagnetic conditions. MURPHREE *et al.* (1982) reached similar conclusions on the basis of ISIS 2 auroral images recorded during periods of northward IMF.

Using images of the total auroral region recorded at few-minute intervals by the auroral imager on DE-1, FRANK *et al.* (1982, 1986) drew attention to the fact that sometimes during quiet geomagnetic conditions the polar cap is apparently spanned by a single prominent sun-aligned arc (transpolar arc) so that the total auroral pattern resembles the Greek letter, θ. They named this configuration, which can sometimes prevail relatively unchanging for an hour or more, a "theta aurora." Field and particle measurements on field lines above the transpolar arc (the theta bar) strongly suggested that those field lines are closed through the plasma sheet boundary layer, implying, possibly, that each lobe of the tail is bifurcated at these times. Another possibility is that the theta bar is a bright poleward-most arc of the evening or morning auroral oval expanded far into the polar cap, possibly implying a gross dawn-dusk asymmetry or tilting of the plasma sheet. PETERSON and SHELLEY (1984) found some tentative support for this latter interpretation in analyzing ion composition data acquired by DE-1 during its flight over a theta aurora that was studied previously by FRANK *et al.* (1982).

Surveying DE-1 images, HONES *et al.* (1989) found that another auroral distribution, the "horse-collar aurora," is quite commonly recorded during geomagnetic quiescence. This pattern features an arrowhead-like polar cap with its narrow end pointed toward the sun and having quite sharply defined dawn and dusk boundaries. In fact, the dawn and/or dusk boundary is often marked by a bright bar spanning the auroral oval roughly in the noon-midnight direction. The regions (called "webs") between the polar cap boundaries (bars) and the dawn and dusk sectors of the auroral oval are typically filled in with diffuse-appearing emissions that are less intense than that from the bars or the oval. At times when one of the bars is prominent and the neighboring diffuse region (web) is faint, the total pattern can closely resemble a theta aurora. The horse-collar aurora clearly resembles an auroral oval with much-expanded morning and evening sectors. Thus, its tendency to evolve sometimes into a theta-like pattern may be some indication that the theta aurora, too, is a consequence of such poleward expansion (cf. CRAVEN *et al.*, 1991).

The theta and horse-collar auroras hold clues to the nature of the solar wind-magnetosphere interaction with northward IMF as to whether, tor example, this interaction causes lobe bifurcation or tilting of the plasma sheet or both. It is thus important to try to determine how these auroral patterns are connected to outer magnetosphere regions using as correct a model as is available. BIRN *et al.* (1991) and ELPHINSTONE *et al.* (1991), working with the TSYGANENKO (1987) model, have noted that the arrowhead-shaped polar cap of the horse-collar aurora closely resembles mappings of the open-closed field line boundary of that model, with the bright "bars" along the sides of the polar cap corresponding to the separatrix layers. The fainter "web" regions between the bars and the oval of the horse-collar pattern connect to the low-latitude boundary regions all along the flanks of the tail.

With some knowledge of the possible magnetic interconnection between the auroras and the outer magnetosphere regions thus established, it is next important to examine the particles, plasma, and fields in the ionosphere above the auroras in an effort to understand the processes in the outer magnetosphere which are the ultimate cause or the auroras. This paper is such a

study. It began with a search for cases in which a horse-collar pattern was imaged by DE-1 at times when its companion satellite, DE-2, passed over the auroral region while measuring the particles, fields, and plasma flows. We found six examples of this that occurred in the Fall of 1981. In this paper we report the observations in the one of those cases where DE-2 passed most directly along the dawn-dusk axis of the oval so that conditions over the main features of the pattern could be best observed. These simultaneous measurements allow the detailed relationships between the ionospheric particle and field measurements to be examined in the context of a larger global scale distribution of the aurora seen from DE-1.

2. Observations

We begin by showing in Fig. 1 a sequence of eight consecutive 12-minute images of the northern hemisphere auroral region taken at FUV wavelengths (123–155 nm) by the Spin-Scan Auroral Imager on DE-1 (FRANK *et al.*, 1981). These images show a contracted oval with emission features in the dawn and dusk sectors expanded into the high-latitude region. This pattern has been referred to as the "horse-collar aurora" (HONES *et al.*, 1989). In this sequence the web and bar features of the horse collar are rather well-defined on the dawn side, whereas the dusk side bar feature does not begin to appear until the sixth flame of the sequence. The general pattern, however, is present throughout the entire 96-minute sequence.

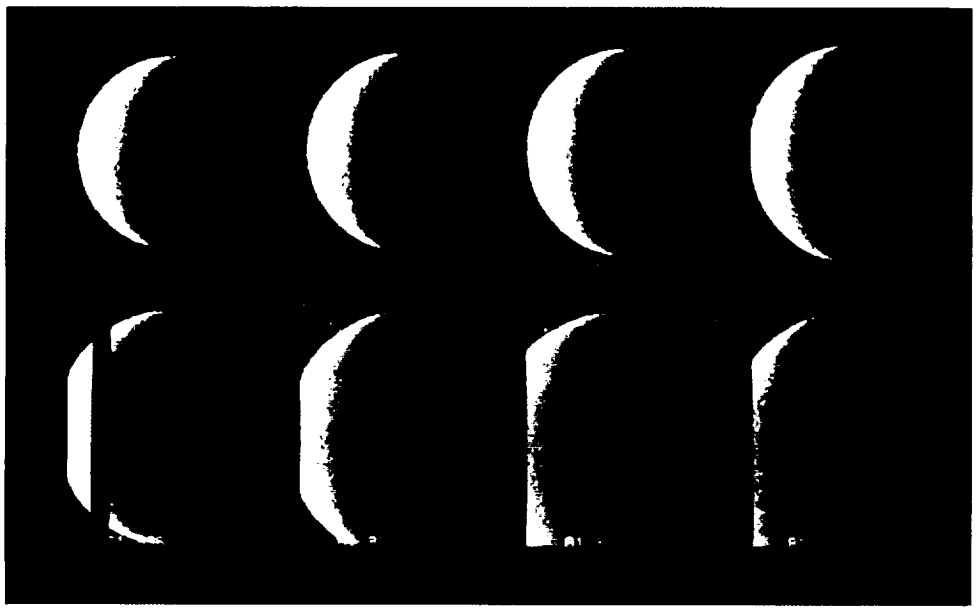

Fig. 1. Sequence of eight consecutive 12-minute images of the northern hemisphere auroral region taken with the Spin-Scan Auroral Imager (SAI) on DE-1. The sequence began at 1421 UT on day 336 (December 2) of 1981 during an interval of relative magnetic quiet between two substorms, and illustrates the general features of a "horse-collar" auroral pattern which persisted for the entire 96-minute sequence. The pass band for these images was 123–155 nm for which the principal auroral emissions are from atomic oxygen (130.4–135.6 nm) and the LBH bands of N_2.

These images were taken on day 336 (Dec. 2) of 1981 beginning at 1421 UT during an interval of relative magnetic quiet between two small substorms. In Fig. 2 it is seen that AE was low (<58 nT) and Dst was negative, with an hourly averaged value of 8 nT between 14 and 15 UT. As measured by ISEE 1 at 1425 UT (GSE coordinates +10.9, 18.5, and 4.4 R_E), B_z was positive (8.8 nT), B_x was positive (11.4 nT), and B_y was negative (4.0 nT). K_p was 2 during the time of the pass.

The lower altitude DE-2 satellite passed over the northern high-latitude region as the first image of Fig. 1 was being made. The DE-2 electron differential measurements at 44° pitch angle are shown in Fig. 3 along with the optical image from DE-1 and an overlay of the DE-2 orbit mapped to 120 km altitude. In general, the optical and particle measurements agree very well. In the electron data, the lowest latitude regions contain broadly peaked spectra in the several hundred eV to few keV range and are characteristic of the diffuse aurora or CPS (WINNINGHAM *et al.*, 1975). The equatorward boundaries of these regions, at 1417:40 UT (62.3° IL) on the dawn side and at 1430:30 UT (65.2° IL) on the dusk side, agree to less than half a minute (1.7° IL) with the optical boundaries. Poleward of 1420:40 UT (72.7° IL) on the dawn side and 1428:00 UT (75.6° IL) on the dusk side, the electron spectrogram often displays sharp spectral peaks at energies of tens to hundreds of eV, indicating acceleration of the population along the field line to the energy of the spectral peak. As we shall see below, these enhancements are associated with gradients in the plasma flow and magnetic field perturbations.

It is clear that the optical emissions are associated with electrons having both the quasi-thermal and the peaked spectra. On the dawn side, for example, emissions are seen between about ~1418 and ~1423 UT, an extent in latitude of 16.6° IL. We note that the relatively bright optical feature crossed by DE-2 just before 1423 UT is associated with the electron energy flux enhancement that peaks at 1422:50 UT. The electrons observed between 1423:40 and 1424:50 UT are mostly polar rain electrons which typically show a Maxwellian peak at ~100 eV. A few small enhancements that produce no detectable emissions are also present in this interval. The dark region seen in the image between ~1423 and 1425 UT includes this region of low intensity polar rain. The dusk-side emissions are less intense and appear to have a poleward "edge" near minute 1425 (83.7° IL). Thus the duskside emissions cover 18.5° of invariant latitude.

The particle precipitation features and electrodynamic properties of the ionospheric plasma are examined in more detail in Fig. 4. The panels show the precipitating electron number flux, the ion drift velocity perpendicular to the satellite track, the transverse magnetic field perturbation, and the electrostatic potential plotted as functions of time. Also shown are some of the locations of emission features seen in the image and described previously. We note that a number flux threshold peak of ~10^9 cm $^{-2}$s $^{-1}$ can be used to distinguish precipitation events that will produce sufficiently intense emission to be seen by the imager. Within the dark region the discrete precipitation features fall below this threshold. We also see that across the entire pass, almost all enhancements in the precipitating electron number flux are associated with gradients in the ion drift velocity. Each gradient is such that, as the spacecraft moves from dawn to dusk, the antisunward flow speed decreases or the sunward flow increases. The association between regions of negative divergence in the dawn-dusk component of the electric field (derived from the cross-track ion drift measurements) and enhancements in the precipitating electron number flux exists over a range of spatial scales. These correspond to a few seconds (~10's of kilometers), as at 1421:28 1421:34 UT, to tens of seconds (~100's of kilometers) as at 1422:40 1423:05 UT. Comparison of the particle and ion drift velocity data

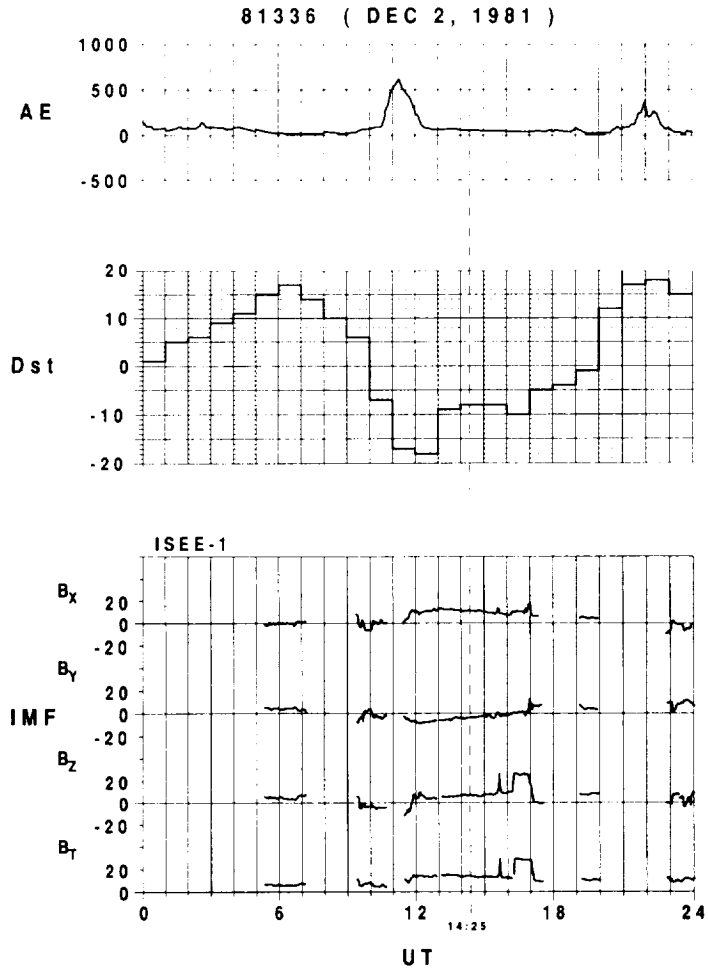

Fig. 2. *AE*, *Dst*, and IMF data for day 336 (Dec. 2) of 1981. The dashed line at 1425 UT is the time near the middle of the DE-2 pass over the polar cap.

with the magnetic field perturbation transverse to the satellite track shows that gradients in the ion drift and in the magnetic field are generally collocated: i.e., a decrease in the antisunward ion drift speed of the third panel of Fig. 4 corresponds to a decrease in ΔB_z in the first panel. (On the DE spacecraft the transverse (z) axis is normal to the orbit plane and positive eastward).

Gradients in the magnetic field perturbation corresponding to an upward field-aligned current are seen to be associated with regions of negative divergence in the dawn-dusk electric field and enhancements in the precipitating electron flux. It is thus most likely that each of these events is electrodynamically self consistent with an approximately uniform height-integrated ionospheric conductivity. In such a case the negative divergence in the electric field requires an upward field-aligned current carried by precipitating electrons that do not appreciably affect the ionospheric conductivity.

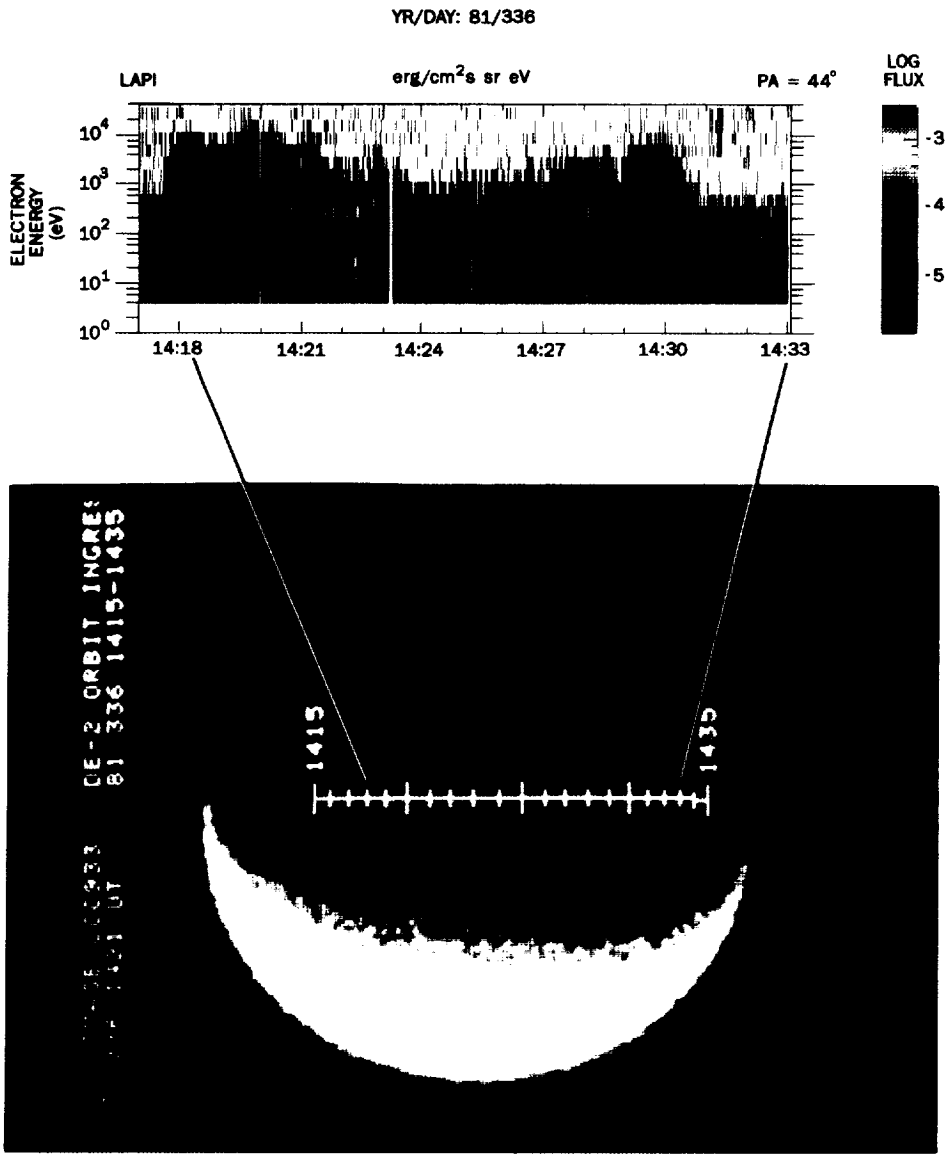

Fig. 3. The 12-minute SAI UV image beginning at 1421 UT of day 336 (Dec. 2), 1981, compared with LAPI measurement of electrons at 44° pitch angle. The foot of the DE-2 field line at 120 km is plotted into the image with universal time minutes shown for reference to the electron spectrogram.

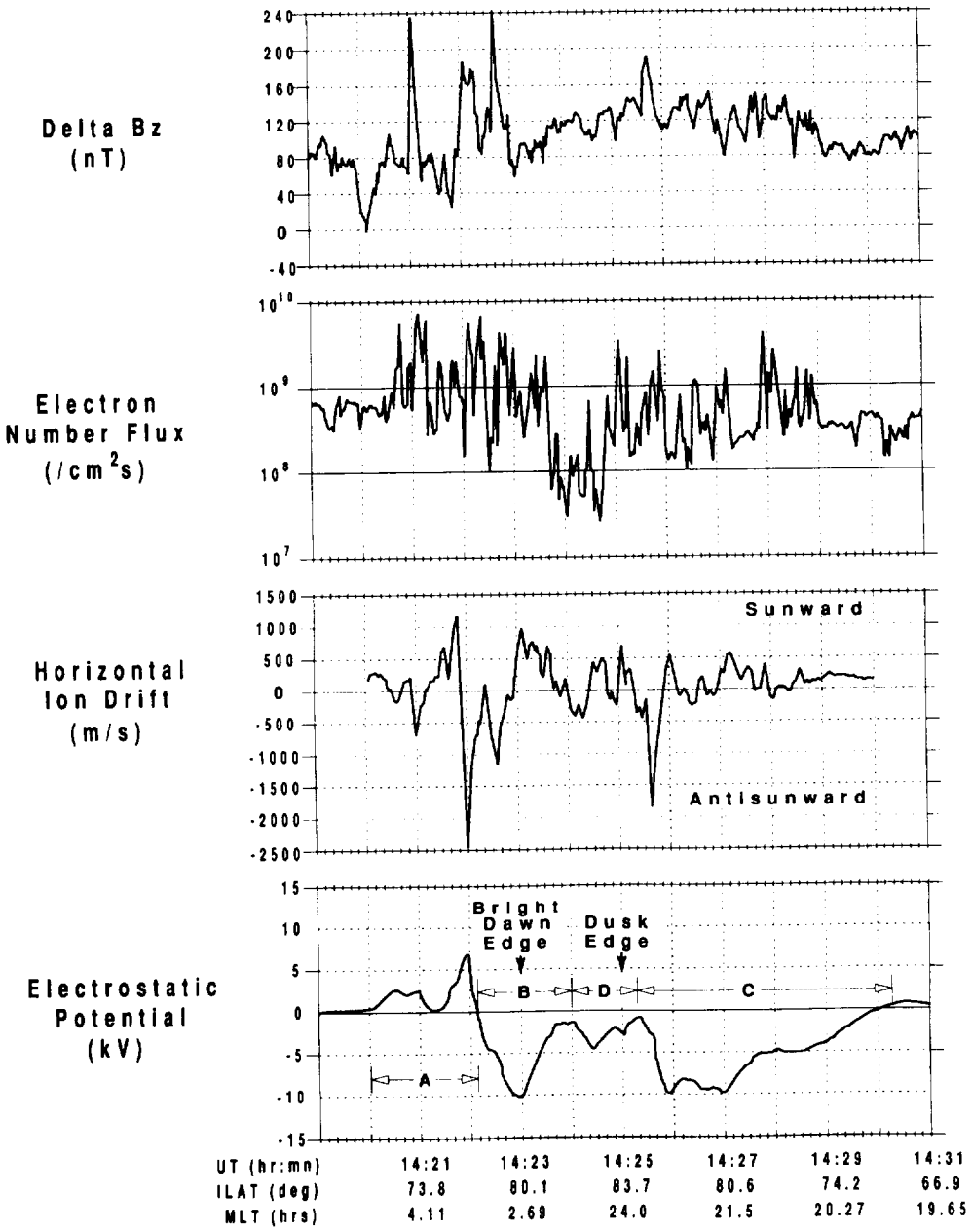

Fig. 4. Field and particle measurements of DE-2 showing magnetometer measurements of ΔB_z, number and energy fluxes of precipitating electrons, and horizontal ion drifts perpendicular to the satellite track. Gradients in the magnetic field perturbation corresponding to an upward field-aligned current are associated with regions of negative divergence in the electric field (i.e. antisunward to sunward flow) and enhancements in the precipitating electron flux. The lower panel shows the electrostatic potential distribution obtained by integrating the electric field along the DE-2 track. Also shown in this panel are the dawn and dusk inner edges of the horse-collar pattern and large-scale potential regions A-D.

We note that the regions of negative and positive divergence in the electric field may involve reversals in the flow direction or simply changes in the sunward or antisunward flow speed. In order to place these gradients in a perspective that includes the flow configuration on spatial scales of 1000 km or more, we will construct a picture of the global ionospheric convection pattern accompanying these data. Here we assume that the convective motion of the plasma may be represented by an electrostatic potential distribution. A signature of the distribution is obtained by integrating the electric field along the satellite track, which is derived from the ion drift velocity transverse to the satellite track. This distribution is shown in the lowest panel of Fig. 4, where we identify one region of positive potential (labeled A) and a large region of negative potential within which there are two major sub-regions of large negative potential (B and C). An additional sub-region of negative potential, labeled D, with a smaller absolute value, but comparable spatial scale, is also seen. It is clear that the spacecraft encounters plasma flow at the same potential at least four times while traversing the high latitude region. Comparison of the features in Figs. 3 and 4 shows that electron precipitation structures and discrete optical emission features appear at or near local minima in the potential distribution. These can correspond to minima within the larger scale regions of positive and negative potential, as at ~1421:15 UT, or they may correspond to the extreme minima of the large scale regions of negative potential themselves, as at 1423 UT. This one (at 1423 UT) is, in fact, the dawnside bright edge of the dark region and marks the extreme minimum in potential of region B. Although on the dusk side the edge of emissions is not very well defined, it appears to be associated with the small minimum in region *D* at ~1425 UT. We also note that two other small minima exist near zero potential within the dark region, one at ~1423:50 UT and one at 1424:24 UT. These correspond to the particle precipitation enhancements seen by DE-2, but do not constitute sufficient energy input to produce detectable emission. On the dawn side, the A cell corresponds approximately with the dawn auroral oval, but includes some of the web emissions extending further poleward. On the dusk side the extended, negative C cell includes the auroral oval plus the web emissions all the way up to the dusk inner edge.

3. Large Scale Convection Pattern

Two factors must be considered in suggesting a large scale convection pattern for this B_z-north case. First, the IMF lies predominantly in the *xz*-plane: a condition most likely to produce multiple cell patterns (see MAYNARD *et al.*, 1990). Second, the region of negative potential extends across the noon-midnight meridian even though the B_y-component is negative (cf. HEPPNER and MAYNARD, 1987). We show in Fig. 5 a multicell convection pattern consistent with the cross-track flows and potential regions of Fig. 4 and the emission features of Fig. 3. These emission features and the DE-2 track are shown for reference. In the pattern, the dawnside auroral region (cell A) encompasses a region of sunward flow at low latitudes and a region of antisunward flow at higher latitudes. Somewhat further poleward and still on the dawn side, DE-2 crosses the bright dawnside high-latitude edge of emissions which is collocated with a flow reversal (antisunward to sunward as the spacecraft moves dawn to dusk). Cell B, containing this bright arc, is drawn as a separate cell (solid lines) in a manner consistent with the flows associated with potential region B of Fig. 4. This cell has sunward flow in the poleward region interior to the horse collar (unshaded). The sunward flow region of cell C, the duskside counterpart of cell A, is associated with the low-latitude diffuse auroral precipitation in that sector. We point out here that at higher latitudes, in the region interior to

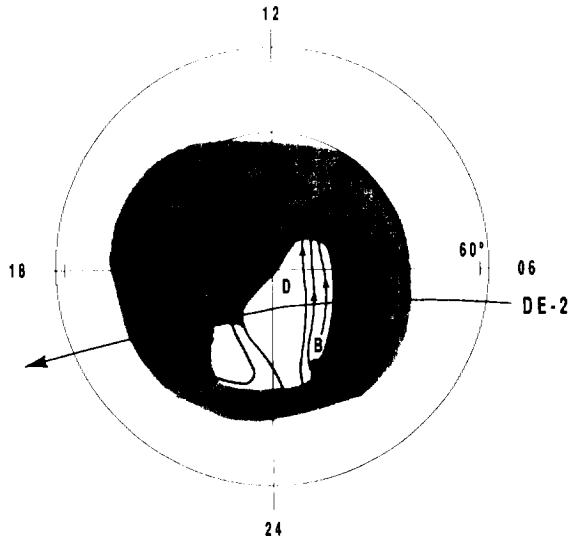

Fig. 5. Multi-cell convection pattern consistent with the DE-2 plasma flow measurement and emission features. The DE-2 track is shown for reference.

the horse collar, Fig. 4 shows a small region of sunward convection bordered on each side by small regions of antisunward convection (i.e. between 1424:00 UT and 1425:04 UT in Fig. 4). The transverse flows measured along the satellite track in this region are weak, and for clarity we have chosen not to draw in a separate cell in the *D* region. The electron density drops slightly in this region, which is consistent with a region of near-stagnant flow as shown here. A small local convection cell circulating only within that region and existing in a steady state would have produced a significant density depression (MAYNARD *et al.*, 1990). From the data it is not possible to determine if the negative potential regions *B* and *C* are connected in the midnight or dayside auroral regions forming a large distorted cell. We have chosen to show them as separate, emphasizing that the cells most likely have different driving sources in the magnetospheric system.

4. Discussion

The horse-collar aurora pattern clearly defines (i.e. surrounds) a region in the ionosphere at the highest latitudes that is relatively darker than the adjacent emission regions. In this example, the dawn side of the dark region is defined by the bright arc forming the "bar" feature of the pattern (HONES *et al.*, 1989). It seems reasonable that this bright feature, which extends to the dayside, indicates a boundary between the open and closed field lines. This assertion is supported to some extent by the LAPI energetic particle detectors (G-M tubes at 0° and 90° responding primarily to electrons of $E > 35$ keV), which show greater flux at 90° than at 0° in the precipitation feature as far poleward as the bright dawnside feature at ~1421 UT (data not shown) and by the modeling studies of BIRN *et al.* (1991) and ELPHINSTONE *et al.* (1991). We then associate the dark region with open field lines. Interpreting the ionospheric flow as an instantaneous electrostatic potential distribution, we see that a large part of the dark region (i.e.

at least the dawn half) contains sunward flow on these open field lines. Ionospheric plasma on these field lines circulates in the manner shown in cell B, eventually flowing antisunward on the dawn side of the bright arc. This cell has the characteristics of the narrow, high-latitude dawnside "collapsed" cell of POTEMRA *et al.* (1984). Such a cell was inferred from electric and magnetic field observations of dayside crossings of the polar cap during times of northward IMF. It was based on the observation of strong flow reversals and associated field-aligned currents and occurred on the dawn (dusk) side of the northern polar cap for moderately negative (positive) values of B_y. Such cells have limited extent in the dawn-dusk dimension and are elongated in the noon-midnight (sun-aligned) direction (ZANETTI *et al.*, 1984; CARLSON *et al.*, 1988). In the present study, the spatial extent of the sunward and antisunward flow regions of the B cell is indicated by the spatial coherence of the bright optical emission associated with it.

In this horse-collar emission pattern, the bright dawnside emission feature is associated with a strong gradient in the antisunward ionospheric plasma flow; i.e., it marks a region in which the divergence of the electric field along the track is negative (1422:40–1423:05 UT). These observations are consistent with results of other studies showing that during IMF north intervals, the most intense outward flowing NBZ currents occur on the dawnside of the polar cap regardless of the IMF B_y direction (ZANETTI *et al.*, 1984; POTEMRA *et al.*, 1984). Thus in a more general context the sharpness of the inner edges (i.e., the "bars") of a horse-collar aurora will depend on the size of the gradients in the electric field; and on the dawnside, the magnitude of the gradient will determine the brightness of the emission feature at the edge. Some observations (GUSEV and TROSCHICHEV, 1986) and modeling (CORNWALL, 1985; REIFF and BURCH, 1985) have associated dawnside polar cap arcs in the northern (southern) hemisphere with negative (positive) IMF B_y. Our observations of the dawn edge feature as well as the feature observed at ~1421 UT are consistent with these findings. In this case B_y was negative during this DE-2 pass and for three hours previous.

Although a more complete mapping of the features of this auroral form into the magnetosphere must await the study of other cases, we can obtain some understanding of possible source regions in terms of mapping studies already carried out. BIRN *et al.* (1991) have shown that the arrowhead shape of the inner edges of the horse-collar pattern comes directly from mapping the last closed field lines of the TSYGANENKO (1987) long model down to the auroral ionosphere. Although the Tsyganenko model is a "closed" model, the last closed field lines were defined operationally by BIRN *et al.* (1991) as those which cross the equatorial plane at -70 R_E. The elongated and pointed shape of the polar cap is more pronounced for low K_p values. The study suggests that the "bars" of the horse-collar pattern map to the separatrix layers (or plasma sheet boundary layers) extending to the distant X-line while the "web" regions map to the low-latitude boundary regions along the flanks of the magnetosphere, which are possibly, but no necessarily, identical with the low-latitude boundary layers. Another study by ELPHINSTONE *et al.* (1991), comparing mappings of the TSYGANENKO (1987) long model with Viking images, finds similar results. In the Elphinstone *et al.* paper, color coded regions in the auroral ionosphere are mapped not only to the equatorial plane, but also into the *yz* GSM plane at specified distances down the tail.

Based on the above studies (see Fig. 1 of BIRN *et al.* (1991) and Plate 1 of ELPHINSTONE *et al.* (1991)), we show in Fig. 6 a cartoon of the magnetospheric *yz* plane at a location roughly 40 R_E down the tail. The view is toward the earth. The figure shows a thickened plasma sheet (PS), a lobe region (LOBE) containing the open field lines, a plasma sheet boundary layer

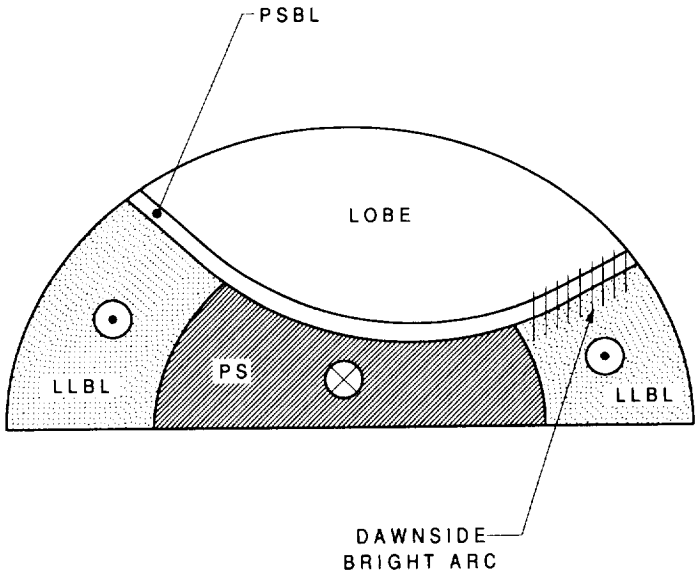

Fig. 6. Sketch of the magnetospheric yz plane at a location roughly 40 R_E down the tail, based mainly on the work of BIRN *et al.* (1991) and ELPHINSTONE *et al.* (1991). The view is toward the earth and shows the bright dawnside arc mapping to the boundary between open lobe field lines and the dawn low-latitude boundary layer. The plasma sheet is identified with sunward flowing plasma in the dawn and dusk convection cells of Fig. 5, while antisunward flowing plasma in these cells is identified with the low-latitude boundary layers.

(PSBL), and two expanded low-latitude boundary layers (LLBL). The plasma flow directions in and out of the paper are consistent with the flow patterns shown in Fig. 5. The bright dawnside arc (or "bar" feature) probably maps to the boundary between open field lines in the lobe and the dawn low-latitude boundary layer. The lobe region in Fig. 6 contains the field lines that are sunward flowing inside the horse collar in Fig. 5. This must coincide with a radially outward flow in Fig. 6 which implies a more contorted tail than shown in the cartoon. Optical emissions in the dawn and dusk auroral ionosphere are associated with the dawn and dusk low-latitude boundary layers and the plasma sheet. Specifically, the plasma sheet is identified with the sunward flowing plasma in the dawn and dusk convection cells of Fig. 5, while antisunward flowing plasma in those cells is identified with the LLBL regions. Note that the BIRN *et al.* (1991) study found the arrowhead shape of the polar cap to be closely associated with an increase in B_z in the magnetotail from midnight toward the flanks. This variation in B_z corresponds to field aligned currents which are earthward on the dusk side and tailward on the dawn side, a condition that is consistent with more intense electron precipitation and arc emission on the dawn side.

5. Summary and Conclusions

We have studied one configuration of quiet-time auroral pattern, a horse-collar aurora, that was observed during an interval in which the IMF had a large northward component, a moderately negative y-component, and a large positive x-component.

We find very good agreement between UV observations of the DE-1 auroral imager and electron precipitation measured by particle detectors on DE-2. Precipitation features include the quasi-thermal populations of the low-latitude (quiet diffuse auroral) regions, regions of accelerated electron fluxes associated with the magnetospheric boundary layers, and a region of mostly polar rain associated with the dark region interior to the horse collar. Small electron enhancements, not observed by the imager, were observed within this region.

Plasma flow and magnetometer measurements show that electron precipitation occurs where gradients are observed in the antisunward plasma flow and the cross-track magnetic field perturbations. The most prominent optical features and many smaller scale enhancements seen in the electron fluxes occur where the dawn-dusk electric field satisfies the condition, $\nabla \cdot \boldsymbol{E} < 0$. This is the case for the bright dawnside edge feature of the horse collar.

The ionospheric convection pattern associated with this auroral form is dominated by two cells circulating in a manner consistent with an electric field source in the low-latitude boundary layers. A third cell contains the dawn edge arc. The large convection cells have potential differences of 5 to 10 kV across them and have latitudinal extents of more than 10°. Auroral oval precipitation is associated with the low-latitude sunward flow in these cells, while the discrete, lower-energy electron precipitation is associated with the antisunward flow through the boundary layers.

Although it is felt that many of the above observations will apply to the general horse-collar auroral pattern, some variation is to be expected based on the strengths of the flows (electric fields) and the direction of the IMF. A study to determine the extent of this variation is now underway.

Two of us (JRS and EWH) wish to acknowledge very helpful discussions with R. Elphinstone. The work was supported at Southwest Research Institute by NASA guest investigator grant NAG5-1553 and SwRI internal research grant 15-9557, at University of Texas at Dallas by Phillips Laboratory Geophysics Directorate contract F19628-90-K-001 and NASA grants NAG5-305 and NAG5-306, at the Geophysics Directorate of the Phillips Laboratory by AFOSR task 231165, at the University of Iowa by NASA grant NAG5-483, and at Los Alamos National Laboratory by the U.S. Department of Energy through the Office of Basic Energy Sciences. Principal participation by JDC occurred while at the University of Iowa. Research at the University of Alaska was funded in part by NASA grant NAGW-2735.

REFERENCES

BIRN, J., E. W. HONES, Jr., J. D. CRAVEN, L. A. FRANK, R. ELPHINSTONE, and D. P. STERN, Open and closed field line regions in Tsyganenko's field model and their possible associations with horse-collar auroras, *J. Geophys. Res.*, **96**, 3811, 1991.

CARLSON, H. C., R. A. HEELIS, E. J. WEBER, and J. R. SHARBER, Coherent mesoscale convection patterns during northward interplanetary magnetic field, *J. Geophys. Res.*, **93**, 14,501, 1988.

CORNWALL, J. M., Idealized model of polar cap currents, fields, and auroras, *J. Geophys. Res.*, **90**, 3541, 1985.

CRAVEN, J. D., J. S. MURPHEE, L. A. FRANK, and L. L. COGGER, Simultaneous optical observations of transpolar arcs in the two polar caps, *Geophys. Res. Lett.*, **18**, 2297, 1991.

ELPHINSTONE, R. D., D. HEARN, J. S. MURPHREE, and L. L. COGGER, Mapping using the Tsyganenko long magnetospheric model and its relationship to Viking auroral images, *J. Geophys. Res.*, **96**, 1467, 1991.

FRANK, L. A., J. D. CRAVEN, K. L. ACKERSON, M. R. ENGLISH, R. H. EATHER, and R. L. CAROVILLANO, Global auroral imaging instrumentation for the Dynamics Explorer mission, *Space Sci. Instrum.*, **5**, 369, 1981.

FRANK, L. A., J. D. CRAVEN, J. L. BURCH, and J. D. WINNINGHAM, Polar views of the earth's aurora with Dynamics Explorer, *Geophys. Res. Lett.*, **9**, 1001, 1982.

FRANK, L. A. *et al.*, The theta aurora, *J. Geophys. Res.*, **91**, 3177, 1986.

GUSEV, M. G. and O. A. TROSHICHEV, Hook-shaped arcs in the dayside polar cap and their relation to the IMF, *Planet. Space Sci.*, **34**, 489, 1986.

HEPPNER, J. P. and N. C. MAYNARD, Empirical high-latitude electric field models, *J. Geophys. Res.*, 4467, 1987.

HONES, E. W., Jr., J. D. CRAVEN, L. A. FRANK, D. S. EVANS, and P. T. NEWELL, The horse-collar aurora: A frequent pattern of the aurora in quiet times, *Geophys. Res. Lett.*, **16**, 37, 1989.

LASSEN, K. and C. DANIELSEN, Quiet time pattern of auroral arcs for different directions of the interplanetary magnetic field in the y-z plane, *J. Geophys. Res.*, **83**, 5277, 1978.

MAYNARD, N. C., J. J. SOJKA, R. W. SCHUNK, J. P. HEPPNER, and L. H. BRACE, A test of convection models for IMF B_z north, *Planet. Space Sci.*, **38**, 1077, 1990.

MENG, C.-I., Polar cap arcs and the plasma sheet, *Geophys. Res. Lett.*, **8**, 273, 1981.

MURPHREE, J. S., C. D. AUGER, and L. L. COGGER, The instantaneous relationship between polar cap and oval auroras at times of northward interplanetary magnetic field, *Can. J. Phys.*, **60**, 349, 1982.

PETERSON, W. K. and E. G. SHELLEY, Origin of the plasma in a cross-polar cap auroral feature (theta aurora), *J. Geophys. Res.*, **89**, 6729, 1984.

POTEMRA, T. A., L. J. ZANETTI, P. F. BYTHROW, A. T. Y. LUI, and T. IIJIMA, B_y-dependent convection patterns during northward interplanetary magnetic field, *J. Geophys. Res.*, **89**, 9753, 1984.

REIFF, P. H. and J. L. BURCH, IMF B_y-dependent plasma flow and Birkeland currents in the dayside magnetosphere, 2, a global model for northward and southward IMF, *J. Geophys. Res.*, **90**, 1595, 1985.

TSYGANENKO, N. A., Global quantitative models of the geomagnetic field in the cislunar magnetosphere for different disturbance levels, *Planet. Space Sci.*, **35**, 1347, 1987.

WINNINGHAM, J. D., F. YASUHARA, S. I. AKASOFU, and W. J. HEIKKILA, The latitudinal morphology of 10 eV to 10 keV electron fluxes during magnetically quiet and disturbed times in the 2100 0300 MLT sector, *J. Geophys. Res.*, **72**, 3148, 1975.

ZANETTI, L. J., T. A. POTEMRA, T. IIJIMA, W. BAUMJOHANN, and P. F. BYTHROW, Ionospheric and Birkeland current distributions for northward interplanetary magnetic field: Inferred polar convection, *J. Geophys. Res.*, **89**, 7453, 1984.